A Family of Models for Manipulation Planning *

Peng Song† Vijay Kumar‡ J.C. Trinkle§ Jong-Shi Pang♯

†Mechanical & Aerospace Engineering, Rutgers University, Email: pengsong@jove.rutgers.edu
‡GRASP Lab, University of Pennsylvania, Email: kumar@grasp.cis.upenn.edu
§Computer Science, Rensselaer Polytechnic Institute, Email: trink@cs.rpi.edu
♯Mathematical Sciences, Rensselaer Polytechnic Institute, Email: pangj@rpi.edu

Abstract

Manipulation tasks are those that cannot be accomplished without making and breaking contacts. A common requirement of planning algorithms is an ability to hypothesize control actions and then predict the evolution of the system using a mathematical model. This model must capture the physics relevant to the task being planned and do so at an appropriate level of details. In this paper, a collection of time-stepping models suitable for manipulation planning are proposed. The model with the highest fidelity is one that incorporates rigid body dynamics, joint constraints, and contacts with local compliance and Coulomb friction. The idea is to plan tasks starting with the simplest model, upgrading the model and replanning each time a plan is found, until a plan is obtained with the model of desired fidelity. This approach is illustrated through a two-finger grasp acquisition problem.

1 Introduction

One long-standing goal of the robotics research community is to develop robots capable of planning and executing manipulation and grasping tasks with objects of different geometric and material properties. Over 25 years ago several articulated hands were built [1, 2], followed by extensive research on control and planning [3]. Despite this, robot hands have found limited application in service and industrial robotics. The lack of adequate actuator and sensor technologies may have been one reason for this failure. Yet, several recent efforts to build hands [4] have demonstrated how technological limitations can be overcome, without a significant increase in applications. We maintain that the main reason for the lack of progress is our poor understanding of the complexity of mathematical models of manipulation with intermittent contact, and the lack of analytical and computational tools.

Analysis, simulation, and planning of systems with frictional, intermittent contacts are challenging because of the non-smooth nature of the underlying mechanics and because of the "curse of dimensionality" that is associated with mechanical systems with a large number of degrees of freedom. In this paper, we build on the recent results in the analysis and simulation of non-smooth dynamical systems by the authors of this paper [5, 6, 7, 8] and others [9, 10], and develop a hierarchy of task models including quasistatic, and second-order models, with and without local contact compliance. We compare the *feasible sets* in an augmented state space suggested by these models through a two-finger manipulation example.

*This work is supported by the National Science Foundation under Grants DMS-0139715, DMS-0139701, IIS-0413227, and IIS-0413138. See http://cronos.rutgers.edu/~pengsong/publications/SKTPisatp05.pdf for a longer version of this paper.

2 Modeling

The system under consideration is composed of bodies, called "robots," that can be directly controlled, bodies called "objects," that move in response to uncontrollable external forces and contact forces, and bodies called "obstacles," whose configurations are specified functions of time (often obstacle configuration functions are constant). At times during planning it will be necessary to explicitly describe contacts and their transitions from separation to contact and rolling to sliding and *vice versa*. Thus it is essential to understand the stratified nature of the configuration space.

2.1 Configuration space

Denote by q, the configuration of the system, and by $\mathcal{C}$, the space of all configurations ignoring nonpenetration constraints. The subset $\mathcal{C}_{\text{free}}$ is the geometrically accessible portion of $\mathcal{C}$; the set of configurations for which the bodies do not overlap, but could be in contact. If all bodies are smooth, the set of all configurations for which a single contact exists between a given pair of bodies, defines a codimension one variety, or stratum, $\mathcal{C}^i_{\text{free}}$. This stratum is the zero level set of the distance function $\psi_i(q)$ between that pair of bodies. Similarly, a contact between a different pair of bodies defines another stratum $\mathcal{C}^j_{\text{free}}$, while the simultaneous presence of both contacts defines a codimension two stratum $\mathcal{C}^{ij}_{\text{free}} = \mathcal{C}^i_{\text{free}} \bigcap \mathcal{C}^j_{\text{free}}$, formed by the intersection of the two codimension one strata. Thus we see that $\mathcal{C}_{\text{free}}$ is a stratified set. Generically, the lowest-dimensional stratum (zero-dimensional) corresponds to contact at m points, where m is the dimension of the ambient C-space. As each contact breaks, the dimension of the corresponding stratum increases by one.

2.2 State space modeling

Denote by $x = (q,\ \dot{q})$, the state of the system, and by $\mathcal{X}$ the space of all states. The strata of $\mathcal{C}_{\text{free}}$ naturally induce

a partition of $\mathcal{X}$ into n_l non-overlapping operating modes. A mode corresponds to a particular choice of interactions at the contacts (sliding, rolling, breaking) and the dynamics in that mode is governed by by distinct set of differential algebraic equations (DAEs). We define an augmented state space $\mathcal{Z} = \mathcal{X} \times \mathcal{P}$, where $\mathcal{P}$ represents the space of the design parameters p, and the the symbol $\times$ denotes the direct product and elements of $\mathcal{Z}$ are given by $z = (x, p)$. The evolution of this extended state variable with an input u is given by

$$\dot{x} = f_l(x, u, p) \quad (1)$$

$$\dot{p} = 0 \quad (2)$$

Note that we may have variability in (or the ability) to vary initial conditions, $z_0 = (x_0,\, p) \in \mathcal{Z}_0 = \mathcal{X}_0 \times \mathcal{P}$, where $x_0 \in \mathcal{X}_0 \subset \mathcal{X}$. Each mode l corresponds to a particular assignment of contact conditions (rolling, sliding, or no contact) to each contact. Thus, for a system with n_c potential contacts, there are 3^{n_c} discrete modes, each characterized by a set of conditions in state space.

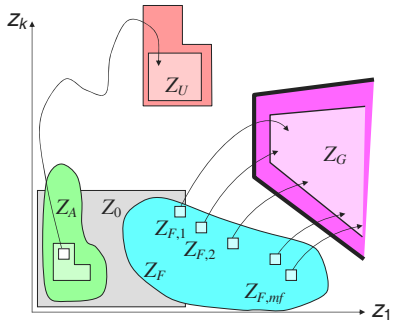

Figure 1: A schematic of the goal set $\mathcal{Z}_G$, the undesirable or unsafe set $\mathcal{Z}_U$, the set $\mathcal{Z}_A$ consisting of points that are guaranteed (regardless of the applied inputs) to lead to the unsafe set, and the feasible set $\mathcal{Z}_F$ consisting of points from which appropriate inputs can steer the system to the goal set.

A generalized manipulation plan consists of actuator input histories and design parameters. The design parameters consist of initial conditions and other parameters that may characterize the system. We are interested in two disjoint sets of points in $\mathcal{Z}$ that characterize significant states of the system. The first set $\mathcal{Z}_G$ is the set of all goal states and parameter values. The second set $\mathcal{Z}_U$ is the set of points that the system must avoid for the successful completion of the task. This is the unsafe set. In addition, we are also interested in determining two disjoint sets of initial conditions and parameters, $\mathcal{Z}_0$, that can be associated with these sets in the following way. The feasible set $\mathcal{Z}_F$ consists of points from which appropriate inputs can steer the system to the goal set $\mathcal{Z}_G$. The set $\mathcal{Z}_A$, are those for which no trajectory passing through them can be steered to $\mathcal{Z}_G$. See Figure 1. It may be difficult to obtain an exhaustive description of $\mathcal{Z}_A$, $\mathcal{Z}_F$, and $\mathcal{Z}_U$. However, even *partial knowledge* of these sets (inset with light shading in the figure) can be important for planning and executing manipulation tasks. This leads to the idea of using a model hierarchy to generate motion plans with different levels of refinement such that the partial knowledge of the sets can be obtained more efficiently using the reduced models in the hierarchy. In the next Section, we present a family of discrete-time models, ranging from the simple, kinematic models to the more complicated, dynamic models with distributed contact compliance.

3 Discrete-Time Models

We derive the dynamic model and then the special cases of the kinematic, and quasistatic models. Instead of writing differential equations for each mode, or discrete state, as in Equations (1) and (2), we will write the model for all modes in a unified framework as a Dynamic Complementarity Problem (DCP) in the spirit of [5, 8].

3.1 Dynamic models

Our full dynamic model uses a distributed compliance for frictional contacts. The key idea of this model is to allow local compliance at the contact patch between nominally rigid bodies. Unlike some penalty methods, the compliant model relies on both normal and tangential compliances to model contact forces and can resolve the inconsistencies with uniqueness and existence.

$$\begin{aligned}
&\epsilon\, M(q^\ell)(\,\nu^{\ell+1} - \nu^\ell\,) = h\,[\,f(t_\ell, q^\ell, \nu^\ell) + \epsilon\, k(t_\ell, q^\ell, \nu^\ell) + \\
&\quad W_{\mathrm{n}}(q^\ell)\lambda_{\mathrm{n}}^{\ell+1} + W_{\mathrm{t}}(q^\ell)\lambda_{\mathrm{t}}^{\ell+1} + W_{\mathrm{o}}(q^\ell)\lambda_{\mathrm{o}}^{\ell+1} + B(q^\ell)u^{\ell+1}\,] \\
&q^{\ell+1} - q^\ell = h\, G(q^\ell)\nu^{\ell+1} \\
&0 \le \lambda_{\mathrm{n}}^{\ell+1} \perp \delta_{\mathrm{n}}^{\ell+1} + \psi_{\mathrm{n}}(q^\ell) + h\, W_{\mathrm{n}}(q^\ell)^T \nu^{\ell+1} \ge 0 \\
&\left(\lambda_{i\mathrm{t}}^{\ell+1},\, \lambda_{i\mathrm{o}}^{\ell+1}\right) \in \underset{(\tilde{\lambda}_{i\mathrm{t}}, \tilde{\lambda}_{i\mathrm{o}}) \in \mathcal{F}_i(\mu_i, \lambda_{i\mathrm{n}})}{\arg\min} \left(s_{i\mathrm{t}}^{\ell+1}\tilde{\lambda}_{i\mathrm{t}} + s_{i\mathrm{o}}^{\ell+1}\tilde{\lambda}_{i\mathrm{o}}\right) \\
&s_{\mathrm{t,o}}^{\ell+1} = W_{\mathrm{t,o}}(q^\ell)^T \nu^{\ell+1} + (\delta_{\mathrm{t,o}}^{\ell+1} - \delta_{\mathrm{t,o}}^{\ell})/h \\
&\lambda^{\ell+1} = K(q^\ell)\delta^{\ell+1} + \frac{C(q^\ell)}{h}\,(\,\delta^{\ell+1} - \delta^{\ell+1}\,)
\end{aligned} \quad (3)$$

where q is the n_q-dimensional vector of generalized coordinates, ν is the n_ν-dimensional vector of generalized velocities, $M(q)$ is the $n_\nu \times n_\nu$ symmetric positive definite mass-inertia matrix, $f(t, q, \nu)$ is the n_ν-dimensional vector containing all non-contact and non-inertial forces, $k(t, q, \nu)$ is the inertial terms that are nonlinear functions of velocity, h is the time step, $\lambda_{\mathrm{n,t,o}}$ are the contact force vectors in the normal direction (labelled n) and the two tangential directions (labelled t and o), $s_{\mathrm{t,o}}$ are the relative tangential velocities between contacting objects, δ is the vector of local deformations at the contact points, and $K(q)$ and $C(q)$ are the stiffness and damping matrices, respectively. A detailed explanation of this model can be found in [5].

The symbol $\perp$ indicates the perpendicularity which means the normal forces at contact i, $\lambda_{i\mathrm{n}}$, can only be non-

zero when the two bodies are in contact which means the normal separation at that contact is zero. In the tangential direction, the contact conditions are formulated by requiring that friction forces maximize the energy dissipation rate over the sets of admissible contact forces computed based on the Coulomb's friction cone model given by

$$\mathcal{F}_i(\mu_i\lambda_{\rm in}) \equiv \left\{(\lambda_{\rm it},\lambda_{\rm io}) : \lambda_{\rm it}^2+\lambda_{\rm io}^2 \le \mu_i^2\lambda_{\rm in}^2\right\}, \quad (4)$$

$W_{\rm n,t,o}$ are the Jacobian matrices defined as

$$W_{\rm n,t,o}(q) \equiv G(q)^T)\left[\frac{\partial \psi_{\rm n,t,o}(q)}{\partial q}\right]^T,$$

where $G(q)$ is a $n_q \times n_\nu$ parametrization matrix relating the system velocity ν to the time-derivative of the system configuration $\dot{q}$ and $\psi_{\rm n,t,o}(q)$ are the constraint functions for all possible contacts in the directions n,t,o, respectively.

Note that we use a positive scalar $\epsilon \in [0,1]$ as a scaling parameter for the inertial terms $M(q)$ and $k(t,q,\nu)$. As $\epsilon \to 0$, the inertial effects are relinquished, and the model degenerates into a quasistatic model. For the dynamic model, $\epsilon = 1$.

Under the assumption of *positive linear independence*, the dynamic **rigid body** model can be obtained, as discussed in [5], by letting the stiffness of the local compliance go to infinity and at same time the local deformations $\delta \to 0$):

$$\begin{aligned}
&\epsilon\, M(q^\ell)(\,\nu^{\ell+1}-\nu^\ell\,) = h\,[\,f(t_\ell,q^\ell,\nu^\ell) + \epsilon\, k(t_\ell,q^\ell,\nu^\ell) + \\
&\quad W_{\rm n}(q^\ell)\lambda_{\rm n}^{\ell+1} + W_{\rm t}(q^\ell)\lambda_{\rm t}^{\ell+1} + W_{\rm o}(q^\ell)\lambda_{\rm o}^{\ell+1} + B(q^\ell)u^{\ell+1}\,]\\
&q^{\ell+1}-q^\ell \;=\; h\,G(q^\ell)\nu^{\ell+1}\\
&0 \;\le\; \lambda_{\rm n}^{\ell+1} \;\perp\; \psi_{\rm n}(q^\ell) + h\,W_{\rm n}(q^\ell)^T\nu^{\ell+1} \;\ge\; 0\\
&\left(\lambda_{\rm it}^{\ell+1},\,\lambda_{\rm io}^{\ell+1}\right) \in \underset{(\tilde\lambda_{\rm it},\tilde\lambda_{\rm io})\in\mathcal{F}_i(\mu_i,\lambda_{\rm in})}{\arg\min} \left(s_{\rm it}^{\ell+1}\tilde\lambda_{\rm it} + s_{\rm io}^{\ell+1}\tilde\lambda_{\rm io}\right)\\
&s_{\rm t,\,o}^{\ell+1} = W_{\rm t,\,o}(q^\ell)^T\nu^{\ell+1}
\end{aligned} \quad (5)$$

For dynamic, rigid-body models, $\lambda_{\rm n,t,o}$ are n_c-dimensional vectors, and $W_{\rm n,t,o}(q)$ are $n_\nu \times n_c$ matrices, where n_c is the total number of contacts. For compliant contact models, the dimensions of these forces and Jacobians are related to the compliance model being used. The right-hand expressions in the model are approximated by a semi-implicit scheme. We can also employ a θ-rule, whereby the differential variables q and ν are evaluated at some intermediate time instances in the respective subintervals determined by the scalar $\theta \in [0,1]$, with $\theta = 1$ indicating a fully implicit time-stepping scheme.

3.2 Quasistatic models

A **quasistatic** model is naturally obtained by allowing the scaling parameter of inertial terms $\epsilon \to 0$.

$$\begin{aligned}
&0 = h\,[\,f(t_\ell,q^\ell,\nu^\ell) + B(q^\ell)u^{\ell+1} +\\
&\quad W_{\rm n}(q^\ell)\lambda_{\rm n}^{\ell+1} + W_{\rm t}(q^\ell)\lambda_{\rm t}^{\ell+1} + W_{\rm o}(q^\ell)\lambda_{\rm o}^{\ell+1}\,]\\
&q^{\ell+1}-q^\ell \;=\; h\,G(q^\ell)\nu^{\ell+1}\\
&0 \;\le\; \lambda_{\rm n}^{\ell+1} \;\perp\; \delta_{\rm n}^{\ell+1} + \psi_{\rm n}(q^\ell) + h\,W_{\rm n}(q^\ell)^T\nu^{\ell+1} \;\ge\; 0\\
&\left(\lambda_{\rm it}^{\ell+1},\,\lambda_{\rm io}^{\ell+1}\right) \in \underset{(\tilde\lambda_{\rm it},\tilde\lambda_{\rm io})\in\mathcal{F}_i(\mu_i,\lambda_{\rm in})}{\arg\min} \left(s_{\rm it}^{\ell+1}\tilde\lambda_{\rm it} + s_{\rm io}^{\ell+1}\tilde\lambda_{\rm io}\right)\\
&s_{\rm t,\,o}^{\ell+1} = W_{\rm t,\,o}(q^\ell)^T\nu^{\ell+1} + (\delta_{\rm t,\,o}^{\ell+1} - \delta_{\rm t,\,o}^{\ell})/h\\
&\lambda^{\ell+1} \;=\; K(q^\ell)\delta^{\ell+1} + \frac{C(q^\ell)}{h}\,(\,\delta^{\ell+1}-\delta^{\ell+1}\,)
\end{aligned} \quad (6)$$

The **quasistatic model without compliance** can also be obtained in a similar manner by letting by letting the stiffness of the local compliance go to infinity:

$$\begin{aligned}
&0 = h\,[\,f(t_\ell,q^\ell,\nu^\ell) + B(q^\ell)u^{\ell+1} +\\
&\quad W_{\rm n}(q^\ell)\lambda_{\rm n}^{\ell+1} + W_{\rm t}(q^\ell)\lambda_{\rm t}^{\ell+1} + W_{\rm o}(q^\ell)\lambda_{\rm o}^{\ell+1}\,]\\
&q^{\ell+1}-q^\ell \;=\; h\,G(q^\ell)\nu^{\ell+1}\\
&0 \;\le\; \lambda_{\rm n}^{\ell+1} \;\perp\; \psi_{\rm n}(q^\ell) + h\,W_{\rm n}(q^\ell)^T\nu^{\ell+1} \;\ge\; 0\\
&\left(\lambda_{\rm it}^{\ell+1},\,\lambda_{\rm io}^{\ell+1}\right) \in \underset{(\tilde\lambda_{\rm it},\tilde\lambda_{\rm io})\in\mathcal{F}_i(\mu_i,\lambda_{\rm in})}{\arg\min} \left(s_{\rm it}^{\ell+1}\tilde\lambda_{\rm it} + s_{\rm io}^{\ell+1}\tilde\lambda_{\rm io}\right)\\
&s_{\rm t,\,o}^{\ell+1} = W_{\rm t,\,o}(q^\ell)^T\nu^{\ell+1}
\end{aligned} \quad (7)$$

3.3 Kinematic and Geometric models

The **kinematic model** can be generated by eliminating $f(t,q,\nu)$ and λ. We have to decompose ν into *controllable speeds* (*i.e.* the control inputs), u, and speeds that are determined by the kinematic constraints.

$$\begin{aligned}
&q^{\ell+1}-q^\ell \;=\; h\,G(q^\ell)\nu^{\ell+1}\\
&\nu^{\ell+1} = \begin{pmatrix} u^{\ell+1}\\ v^{\ell+1}\end{pmatrix}\\
&v^{\ell+1} \in \underset{\psi_{\rm n}(q^{\ell+1})\ge 0}{\arg\min}\, \|v^{\ell+1}\|^2
\end{aligned} \quad (8)$$

Note that for the dynamic models (both rigid and compliant), the inputs u are forces. In the kinematic model, u are the controllable speeds. We use a minimum principle to determine the speeds that are passive. For quasistatic models (both rigid and compliant), the inputs are the controllable speeds that determine the evolution of motion, similar to the kinematic model.

The geometric models are simply described by a set of non-penetration constraints that depends only on the geometry. Globally they are represented semi-algebraic sets constructed with distance functions. However when simulating a system over a small time step starting from a geometrically generic configuration, the non-penetration conditions can be expressed as a conjunction of non-negativity constraints on the relevant distance function:

$$\psi_{\rm n}(q^{\ell+1}) \ge 0. \quad (9)$$

4 Grasp Acquisition Planning

In order to illustrate our hierarchical modeling approach, consider the grasp acquisition for the triangular part shown in Figure 2. The two frames of action on the top of Figure 2 show grasp acquisition of the part via the simple strategy of surrounding the object with four fingers (left frame), holding the bottom two fingers fixed, and moving the top two fingers downward until they achieve contact on opposite sides of the triangle's peak. As the fingers continue to move, they force the triangle to contact the two fixed fingers. If executed accurately, a *form closure grasp* is achieved (middle frame). However, as shown in the bottom two frames, dynamic effects (impact, friction) and uncertainty (positioning and control errors) can cause this simple grasp acquisition plan to fail (right frame).

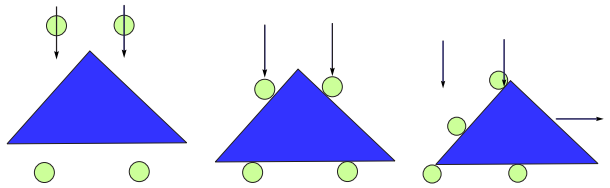

Figure 2: Successful (middle frame) and unsuccessful (right frame) grasp acquisition attempts.

Consider the similar grasp acquisition planning problem with two moveable fingers and a fixed "palm" of infinite length (appearing as finite length) in Figure 3. The simplest model is a geometric model that allows all motions except those that cause interpenetration of rigid bodies. Given that the fingers are small discs and the palm is fixed, the ambient C-space (configuration space) is a stratified space embedded in $\Re^2 \times \Re^2 \times SE(2)$ (the fingers are treated as particles). Since the fingers and triangle can move independently under a geometric model (the triangle need not be pushed by a finger to move), it is possible to find a deterministic plan using, for example, a randomized motion planner to achieve a form closure grasp from any initial configuration.

One can refine the plan by restricting the set of valid plans with a more accurate model. In this example, a kinematic model imposes the restriction that the two fingers can only move vertically; from their fully raised positions ($x_1 = x_2 = 0$) to contact with the palm ($x_1 = x_2 = l_6$). For simplicity, let us also assume that the triangle may only translate horizontally ($-\infty < x_3 < \infty$). Under this kinematic model (and if the fingers are modeled as points), the ambient C-space is $\Re^3$ and $\mathcal{C}_{\text{free}}$ is a solid of infinite length along the x_3-axis with constant square cross section in planes perpendicular to the x_3-axis. Only in the region drawn in Figure 4 ($-1.5 < x_3 < 1.5$) is the cross section not square. In this picture, each of the facets of polyhedron bounding $\mathcal{C}_{\text{free}}$ is a stratum of codimension one. Some of the strata correspond to finger motion limits, but four of them correspond to contact between the fingers and the two upper faces of the triangle. The codimension two stratum highlighted as a blue edge (solid line joining $(1, 2, -0.5)$ to $(2, 1, 0.5)$) corresponds to fingers contacting the triangle's edges on either side of the peak. For this geometry, the blue codimension two stratum is the *goal set* projected onto C-space, the set of all form closure grasps. Since the kinematic model incorporates no contact mechanics, form closure acquisition plans exist for arbitrary initial configurations, since the triangle can move without being pushed.

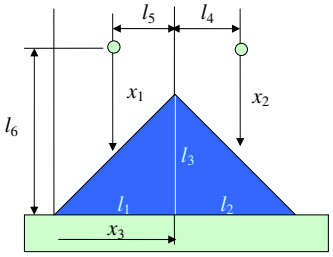

Figure 3: An example of using two fingers to manipulate a triangle sitting on the horizontal plane.

We next refine again, upgrading from a kinematic to a quasistatic model, which in addition to requiring satisfaction of the kinematic constraints, also imposes equilibrium conditions at every point along any motion trajectory. This dramatically prunes the space of feasible plans, since now contact is required to move the triangle. The family of trajectories shown in Figure 4 (a) were generated using a quasistatic model assuming no friction on the palm and Coulomb friction at the other contacts, with coefficient μ less than 1. The quasistatic controller was assumed to move the fingers downward at constant, but not necessarily equal, speeds. Starting from the origin of C-space, we see that form closure is guaranteed as long as the ratio of the fingers' speeds is between approximately 0.7 and 1.4. If the speed ratio is outside these bounds, then the grasp acquisition attempts fail. In Figure 4(a) these trajectories (dotted lines) move to the edges defined by the circled vertices and eventually halt at either the point $(2, 2, 1.5)$ or $(2, 2, -1.5)$ indicating that the fingers have moved down to the palm, but the triangle has slipped out to the left or right.

We now consider a further refinement with full dynamics and with local contact compliance (implicitly defining a frictional impact law with a non-zero coefficient of restitution). The fingers are position-controlled with a proportional controller. The resulting trajectories using the dynamic model with inelastic and elastic impact behavior are given in Figures 4(b) and (c), respectively. The similarity between Figure 4(a) and (b) suggests that in this particular example, if impacts between the fingers and the triangle can be ignored, then the quasistatic model is a good approximation of the dynamic model. When the effective coefficient of restitution is nonzero, the feasible set shown in Figures 4(c) becomes smaller comparing with Figure 4(a,b). This is because when one finger contacts the triangle first at high speed, the impact would cause the triangle jump quickly to the other side, escaping the grasp before the second finger could stop it, thus

narrowing the feasible region(as seen in Figure 4(c)). However, this is only true if we ignore the dynamics of the fingers. If we expand the dynamic model to include dynamics of the two fingers, then, due to significant compliance and friction, the finger that makes contact first gets slowed down or bounced backwards after the collision. So the second finger has more time to reach the other side of the triangle. In this case, the feasible set actually gets expanded comparing with that of using the quasistatic model, as seen in Figure 4(d). In this case, the fingers moved under a force control scheme derived from a quadratic, attractive-well type of potential field centered on the edge of the triangle.

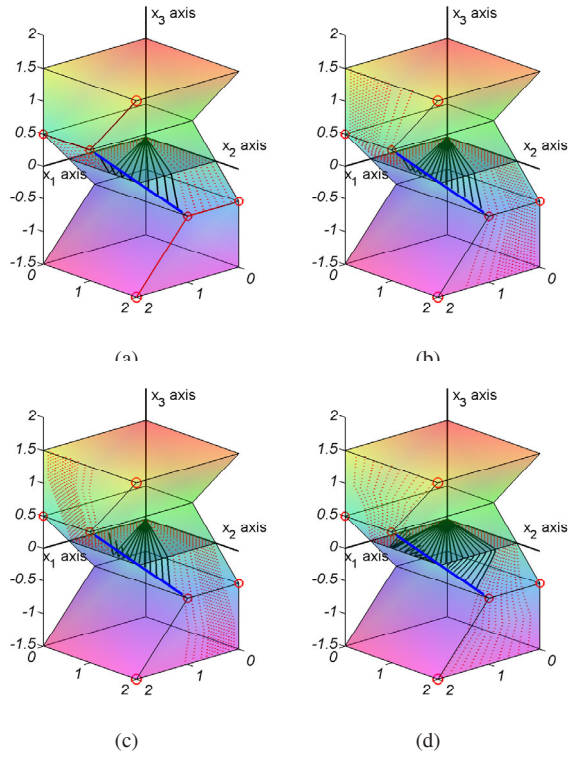

Figure 4: Trajectories and $\mathcal{C}_{\text{free}}$ of the triangle computed by using (a) the quasistatic model; (b) the dynamics model with plastic impacts; (c) the dynamics model with elastic impacts; (d) the complete dynamic model including the dynamics of the two fingers. The following parameters are used in the computation: $l_1 = l_2 = l_3 = 1$, $l_4 = l_5 = 0.5$, $l_6 = 2$. The initial conditions are given by $x_{10} = x_{20} = x_{30} = 0$ and the triangle begins at rest.

Figure 4(b) and (c) are generated by using the dynamic model (3) with different damping coefficients C to achieve different post-impact behaviors. Figure4(a) is generated using the corresponding quasistatic, rigid contact model (7).

For this 2D problem, the dynamic model 3 can be formulated into the following Mixed Linear Complementarity Problem (MLCP) with

$$W_{\text{n}} = \begin{bmatrix} \frac{\sqrt{2}}{2} & -\frac{\sqrt{2}}{2} \end{bmatrix} \text{ and } W_{\text{t}} = \begin{bmatrix} \frac{\sqrt{2}}{2} & \frac{\sqrt{2}}{2} \end{bmatrix}.$$

The generalized coordinate $q = (x_3)$. Other constant parameters include $M = 1$, $h = 10^{-4}$, and $\mu_{1,2} = 0.5$. K is a 4×4 diagonal matrix with all the diagonal entries equal to 10^6. For plastic impacts, C is a 4×4 diagonal matrices with all the diagonal entries set to be 10^4 and C is a zero matrix for elastic impacts. The Jacobian matrices given here only represent the situation where the finger 1 is directly above the left edge of the triangle and finger 2 is above the right one. In this example, because of the geometry of the triangle, the constraint $\psi_{\text{in}}(q)$ is a piecewise linear function of q. In general, $\psi_{\text{in}}(q)$ is piecewise smooth.

Figure 5 illustrates $\mathcal{Z}_F$ and $\mathcal{Z}_U$ in the space of finger speed set points $(\dot{x}_1, \dot{x}_2)$ and finger friction coefficients (μ). For the quasistatic model with finger control as specified above, friction coefficients less than 1, and initial state at the origin, $\mathcal{Z}_F$ is the set of the finger velocity ratios bounded roughly by 0.7 and 1.4 (the green planes). For values of $\mu \geq 1$, the feasible set widens to include the entire first quadrant of the $\dot{x}_1$-$\dot{x}_2$ plane. For the reason explained in the previous paragraph, the feasible set $\mathcal{Z}_F$ gets expanded when we use the dynamic models that consider the dynamics of both the object and the two fingers. As friction increases, the motion of the triangle to the side is further slowed, further expanding the feasible region until it sticks. For larger values of friction, the feasible sets of the quasistatic and dynamic models match (shown in Figure 5). In this case, the set $\mathcal{Z}_A$ can be determined by inspection to be a superset of all points satisfying $x_3 > 0.5$ or $x_3 < -0.5$.

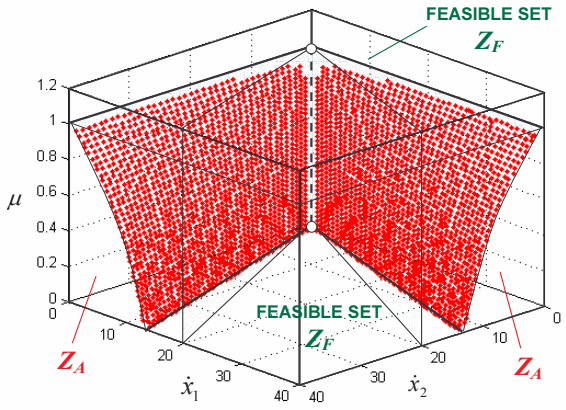

Figure 5: The feasible set $\mathcal{Z}_F$ and the set $\mathcal{Z}_A$ for the quasistatic and dynamic models.

5 Disscussion

Section 3 contains DCP formulations of a collection of models ranging from the simple, kinematic model to the full dynamic, compliant contact model, and more importantly, shows that all of these models sharing a common formalism given by Equation (3). The question to ask is whether they admit a model hierarchy. The following are two possible definitions for model reduction in a hierarchy consisting of all five discrete-time models described in Section 3.

Definition 1 Consider two systems S_1 and S_2 defined as:

$$\dot{x} = f(x, u) \tag{10}$$

and

$$\dot{y} = g(y, v) \tag{11}$$

respectively, where x and y are states, and u and v are inputs. Further, suppose there is a transformation κ that maps x to y:

$$y = \kappa(x).$$

S_2 is a simplification of S_1 (or an approximation of S_1) if for any $\sigma > 0$ and for *all* inputs $v(t)$, there exists a $u(t)$ such that

$$\|\kappa(x^{S_1}(t)) - y^{S_2}(t)\| < \sigma$$

for all $t \in [0, T)$.

Definition 2 A second definition of hierarchy comes from singular perturbation theory in the spirit of [11]. Let x be defined by:

$$x = \begin{bmatrix} y \\ w \end{bmatrix} \tag{12}$$

$$\begin{bmatrix} \dot{y} \\ \epsilon\dot{w} \end{bmatrix} = \begin{bmatrix} f_1(y, w, v) \\ f_2(y, w) \end{bmatrix} \tag{13}$$

Let the solution to $f_2(y, w) = 0$ be given by $w = \kappa(y)$, so that

$$\dot{y} = g(y, v) = f_1(y, k(y), v).$$

If the reduced-order model S_2 is stable, then S_2 can be considered to be a reduction of S_1 as the perturbation parameter ϵ goes to zero.

Table 1 shows which definition of model reduction or approximation the most relevant model pairs satisfy. Some of the simplifications seem to satisfy either Definition 1 or Definition 2, and some neither.

Table 1: Model reduction and approximation

From	To	Hierarchy
Compliant, Dynamic	Rigid, Dynamic	*Def.* 2
Compliant, Dynamic	Rigid, Quasistatic	*Def.* 2
Rigid, Dynamic	Rigid, Quasistatic	*Def.* 2
Rigid, Quasistatic	Kinematic	*Def.* 1

Definition 1 provides an efficient way of manipulation planning. It allows us to generate an initial plan quickly based on the simplified dynamics of S_2 with the assurance that this plan can be refined in successive iterations by upgrading the model to S_2 with a higher resolution along the hierarchy. In general, theoretical guarantees of such a reduction is hard to come by. We leave this for future investigations. Definition 2 is very helpful and sometimes critical [11] in establishing conditions under which solution trajectories from a more complicated, higher-resolution model converges to a simplified, reduced model solution.

6 Summary

The ultimate goal of our research is to be able to automatically generate motion plans (inputs) and designs (initial conditions and parameters) for grasp acquisition, dexterous manipulation, and assembly operations. In this paper, we present a family of models that lend themselves to planning of manipulation tasks. Our approach, which is illustrated by the example in Section 4, is to boot-strap the process with a low-resolution model what will allow us to obtain an initial plan quickly and then refine this plan in successive iterations by upgrading to models with higher resolution and fidelity. In Section 5, we presented two formal definitions that suggest a hierarchical organization of dynamic models for manipulation planning. More importantly, all these models are shown to admit a unified DCP framework, from the simple kinematic model to the full dynamic, rigid contact model, all of which are special cases of an "exact" high-resolution model given by the DCP formulation (3). We are currently working on automated generation of plans for planar microassembly tasks and the design of part feeders for automated assembly.

References

[1] J. K. Salisbury, "Kinematic and force analysis of articulated hands," Ph.D. dissertation, Stanford University Department of Mechanical Engineering, May 1982, reprinted in, Robot Hands and the Mechanics of Manipulation, MIT Press, Cambridge, Massachusetts, 1985.

[2] S. Jacobsen, J. Wood, D. Knutti, and K. Biggers, "The utah/mit dextrous hand: Work in progress," in *Robot Grippers*, D. Pham and W. Heginbotham, Eds. IFS Publications Ltd., UK, 1986, pp. 341–389.

[3] R. M. Murray, Z. Li, and S. S. Sastry, *A Mathematical Introduction to Robotic Manipulation*. CRC Press, 1994.

[4] J. Butterfass, M. Grebenstein, H. Liu, and G. Hirzinger, "Dlr-hand ii: Next generation of a dextrous robot hand," in *icra*, Kyongju, South Korea, 2001, pp. 109–120.

[5] P. Song, J.-S. Pang, and V. Kumar, "A semi-implicit time-stepping model for frictional compliant contact problems," *International Journal for Numerical Methods in Engineering*, vol. 60, pp. 2231–2261, 2004.

[6] D. Stewart and J. Trinkle, "An implicit time-stepping scheme for rigid body dynamics with coulomb friction," in *Proceedings, IEEE International Conference on Robotics and Automation*, 2000, pp. 162–169.

[7] P. Song, J. Trinkle, V. Kumar, and J.-S. Pang, "Design of part feeding and assembly processes with dynamics," in *Proceedings, IEEE International Conference on Robotics and Automation*, May 2004, pp. 39–44.

[8] J. Trinkle, J. Pang, S. Sudarsky, and G. Lo, "On dynamic multi-rigid-body contact problems with coulomb friction," *Zeitschrift für Angewandte Mathematik und Mechanik*, vol. 77, no. 4, pp. 267–279, 1997.

[9] M. Anitescu and F. Potra, "Time-stepping schemes for stiff multi-rigid-body dynamics with contact and friction," *International Journal for Numerical Methods in Engineering*, vol. 55, pp. 753–784, 2002.

[10] J. A. Tzitzouris, "Numerical resolution of frictional multi-rigid-body systems via fully implicit time-stepping and complementarity," Ph.D. dissertation, Department of Mathematical Sciences, The Johns Hopkins University, Baltimore, MD, September 2001.

[11] P. Song, P. Kraus, V. Kumar, and P. Dupont, "Analysis of rigid–body dynamic models for simulation of systems with frictional contacts," *ASME Journal of Applied Mechanics*, vol. 68, pp. 118–128, 2001.